Computational study of the thermal conductivity in defective carbon nanostructures

Zacharias G. Fthenakis and David Tománek[*]

Physics and Astronomy Department, Michigan State University, East Lansing, Michigan 48824, USA

We use nonequilibrium molecular dynamics simulations to study the adverse role of defects including isotopic impurities on the thermal conductivity of carbon nanotubes, graphene, and graphene nanoribbons. We find that even in structurally perfect nanotubes and graphene, isotopic impurities reduce thermal conductivity by up to one half by decreasing the phonon mean-free path. An even larger thermal conductivity reduction, with the same physical origin, occurs in presence of structural defects including vacancies and edges in narrow graphene nanoribbons. Our calculations reconcile results of former studies, which differed by up to an order of magnitude, by identifying limitations of various computational approaches.

I. INTRODUCTION

With increasing performance of microprocessors, rising heat evolution poses a serious problem.[1] To prevent damage, excess heat is conducted away to a heat sink using interconnects with high thermal conductivity. In diamond, which is used for this purpose and which conducts heat by phonons, isotopic impurities reduce its excellent thermal conduction by up to one half.[2,3] The initial prediction that thermal conductivity of perfect carbon nanotubes and graphene monolayers (not graphite) should be similar and even surpass the diamond values[4] was subsequently confirmed experimentally, albeit with a large scatter in the observed values.[5] The added benefit of nanotubes and graphene is their dual role as thermal conductors and active elements in electronic circuits. Unlike in heavier elements, the $^{13}C/^{12}C$ mass ratio does modify the phonon spectra of graphitic nanostructures significantly, causing a large reduction in thermal conductivity of systems with both isotopes.[6,7]

To obtain microscopic understanding of factors limiting thermal conductivity in graphitic nanostructures, we perform large-scale nonequilibrium molecular dynamics (MD) simulations of defective carbon nanotubes, graphene, and graphene nanoribbons. We determine the temperature-dependent thermal conductivity of ^{12}C-based systems as a function of ^{13}C concentration and compare the effect of isotopic impurities to that of divacancies. We show that, depending on temperature, the thermal conductivity of $^{13}C_x{}^{12}C_{1-x}$ nanostructures may be quenched by up to one half with respect to isotopically pure systems. Even at low concentrations, atomic vacancies quench thermal conductance more efficiently than isotopic impurities. Whereas freely suspended graphene monolayers conduct heat almost as well as isolated carbon nanotubes, edge scattering reduces significantly the thermal conductivity of graphene nanoribbons. Our calculations reconcile results of former studies, which differed by up to an order of magnitude, by identifying limitations of various computational approaches.

Since in carbon nanostructures the electronic density of states at the Fermi level is either zero (diamond, graphene) or very small (nanotubes, graphene nanoribbons), thermal transport in these systems is dominated by phonons. According to Fourier law, the thermal conductivity λ is given by the heat current dQ/dt through area A in response to a temperature gradient dT/dz as

$$\frac{1}{A}\frac{dQ}{dt} = -\lambda\frac{dT}{dz} \ . \tag{1}$$

The phonon component of the thermal conductivity, which is dominant, is the product $\lambda = (1/3)c_V v_s \langle l \rangle$, where c_V is the specific heat per volume, v_s the speed of sound, and $\langle l \rangle$ is the phonon mean-free path. Rigid interatomic bonds in both sp^2 and sp^3 carbon structures are responsible for a very high speed of sound v_s and hard phonon modes, which translate into a high Debye frequency and large value of the specific heat c_V. In isotopically pure monocrystalline diamond and carbon nanotubes, the phonon mean-free path $\langle l \rangle$ may approach a large fraction of a micrometer, giving rise to record thermal conductivity values[2,5] as large as ≈40 000 Wm^{-1} K^{-1} near $T ≈ 100$ K.

Since presence of defects, including isotopic impurities and atomic vacancies of different types, can not be avoided in realistic systems, it is imperative to understand their role in thermal conductivity. We expect defects to play only a minor role in changing the speed of sound and specific heat, but to reduce drastically the phonon mean-free path and thus the value of λ. We believe that the large scatter in the observed data[5] comes not only from the extreme difficulty to measure this quantity in excellent thermal conductors, but more importantly due to different types and concentrations of defects in different samples. Since controlling defects on the nanometer scale is nearly impossible experimentally, computer simulations provide a welcome alternative to understand the effect of particular defects on thermal conductivity.

II. METHOD

To simulate computationally the conduction of heat, we make use of large-scale nonequilibrium molecular dynamics (NEMD) simulations,[8–11] which had been used successfully to predict thermal conductivity of nanotubes and graphene.[4] The alternative way to calculate λ using direct MD simulations based on Eq. (1) requires applying a thermostat that maintains a finite-temperature difference ΔT across a finite distance Δz. To prevent artifacts, Δz must be larger than the phonon mean-free path of up to 1 μm, which is computationally impracticable. A second alternative, which does not suffer from this limitation,[12] is based on the Green-Kubo formula[13]

that relates λ to the time-averaged autocorrelation function of the heat flux in the system. As shown earlier,[4] this time average converges very slowly in an equilibrium MD simulation and depends sensitively on the initial conditions, making extensive ensemble averaging a necessary requirement that is computationally extremely demanding for systems of interest here.[14] Due to these problems,[12] thermal conductivity calculations of graphitic nanostructures based on direct MD,[15,16] NEMD,[17] the Green-Kubo formalism,[14,18,19] or the Landauer nonequilibrium Green's function formalism[20,21] have arrived at inconsistent results that differed by up to an order of magnitude and thus need to be revisited.

Our computational approach[8] combines the Green-Kubo formula[13] with nonequilibrium molecular dynamics[9,10] in a computationally efficient manner.[22] The dynamics of the system is driven by forces

$$\mathbf{F}_i = m_i \frac{d^2\mathbf{r}_i}{dt^2} = -\nabla_i U - \zeta m_i \mathbf{v}_i + \Delta\mathbf{F}_i, \qquad (2)$$

which act on individual atoms i. Here, $\mathbf{r}_i$ is the position and $\mathbf{v_i}$ the velocity of atom i with mass m_i.

The first term is the gradient of the total potential energy U of the system, representing the force caused by interatomic interactions. To reduce the unusually high computational requirements, we represent U by the Tersoff bond-order potential,[23] which reproduces well the optimum structure as well as vibration spectra of graphene and related nanostructures.[24] This potential also formally allows a decomposition of the total potential energy into potential energies u_i of individual atoms $U = \sum_i u_i$, which will be of use in the following.

The second term describes a Nosé-Hoover thermostat[25,26] that represents coupling of the system to a heat bath at temperature T. The dynamics of the generalized coordinate ζ of the heat bath is governed by

$$\frac{d\zeta}{dt} = \frac{1}{Q}\left(E_K - \frac{3N-6}{2}k_B T\right), \qquad (3)$$

where E_K is the kinetic energy of the N-atom system and Q the thermal inertia of the heat bath.

The third term is a small fictitious force that acts as a perturbation, driving the system out of equilibrium to generate a heat flux, and is given by

$$\Delta\mathbf{F}_i = \Delta e_i \mathbf{F}_e - \sum_{j\neq i}\mathbf{f}_{ij}(\mathbf{r}_{ij}\cdot\mathbf{F}_e) + \frac{1}{N}\sum_j\sum_{k\neq j}\mathbf{f}_{jk}(\mathbf{r}_{jk}\cdot\mathbf{F}_e). \qquad (4)$$

Here, $\mathbf{F}_e$ is a vector parameter (with the dimension of inverse length) representing the strength of the perturbation. $\mathbf{r}_{ij} = \mathbf{r}_j - \mathbf{r}_i$ and $\Delta e_i = e_i - \langle e \rangle$ is the excess energy of atom i, where $e_i = m_i v_i^2/2 + u_i$ is its instantaneous energy and $\langle e \rangle = 1/N \sum_i e_i$. The quantity $\mathbf{f}_{ij} = -\nabla_i u_j$ represents the contribution to the force on atom i stemming from its interaction with atom j, where ∇_i is the gradient with respect to the position of atom i.

The heat flux in the system is then given by

$$\mathbf{J}(t) = \frac{d}{dt}\sum_{i=1}^{N}\mathbf{r_i}\Delta e_i = \sum_i \mathbf{v}_i \Delta e_i - \sum_i\sum_{j\neq i}\mathbf{r}_{ij}(\mathbf{f}_{ij}\cdot\mathbf{v}_i). \qquad (5)$$

Setting $\mathbf{F}_e = F_e\hat{\mathbf{z}}$, the z component of the heat flux can be obtained using the simplified expression[9,11]

$$J_z = \frac{1}{F_e}\sum_i \mathbf{v}_i \Delta\mathbf{F}_i, \qquad (6)$$

which leads to the thermal conductivity λ along the z direction:

$$\lambda = \lim_{\mathbf{F}_e\to 0}\lim_{t\to\infty}\frac{\langle J_z(\mathbf{F}_e,t)\rangle_t}{F_e T V}. \qquad (7)$$

This approach to determine λ has been shown to be equivalent to that obtained using the Green-Kubo formula,[9,11] yet is computationally much less demanding.[27]

To determine λ in defect-free and defective nanotubes, graphene, and graphene nanoribbons, we integrated the equations of motion using $\Delta t = 0.2$ fs as time step. We used the fifth-order predictor-corrector algorithm[28] for Eq. (2) and the fourth-order algorithm to integrate the coupled Eq. (3). We used $Q = 10$ a.m.u. $\cdot$ Å^2 for the thermal inertial of the thermostat, which allowed for efficient thermalization while not disturbing significantly the dynamics of the system. The number of time steps needed for a reliable time average of the heat flux in Eq. (7) varied depending on the system, the temperature, and the value of $\mathbf{F}_e$. We found that only $500\,000$ time steps were sufficient to reach convergence for $F_e > 10^{-3}$ Å^{-1}, but for smaller values 10^{-5} Å$^{-1} < F_e < 10^{-3}$ Å^{-1}, we used up to 2×10^6 time steps covering a 0.4-ns time period. The estimated 10%–20% error in the extrapolation of our results towards $\mathbf{F}_e \to 0$ is shown by the error bars of λ in Figs. 1–3.

III. RESULTS AND DISCUSSION

A. Thermal conductivity of carbon nanotubes

Our results for the thermal conductivity of perfect and defective (10,10) carbon nanotubes are presented in Fig. 1. We used periodic boundary conditions with a large unit cell containing 400 C atoms, depicted in Fig. 1(d). Focusing first on structurally perfect nanotubes with the isotopic composition $^{13}C_x{}^{12}C_{1-x}$, we present in Figs. 1(a) and 1(b) the thermal conductivity of isotopically pure (^{12}C and ^{13}C) nanotubes and isotope mixtures with $x = 0.05$ and 0.10 in the temperature range up to 600 K. In all systems, the low-temperature behavior of λ is dominated by that of c_V, which, along with λ, approaches zero for $T \to 0$ K and then gradually increases with increasing temperature. After reaching its maximum, which occurs near $T \approx 100$ K in nanotubes, λ decreases again due to the decreasing phonon mean-free path, caused by increasing structural disorder at high temperatures. We find the thermal conductivity to be highest in isotopically pure ^{12}C nanotubes, with isotopically pure ^{13}C nanotubes reaching almost the same value. We represented nanotubes with an isotopic mixture $x = 0.05$ and 0.10 by randomly distributing ^{13}C atoms across the ^{12}C lattice. Our results for these mixtures indicate that for $T < 300$ K, the thermal conductivity may decrease by up to 30% with respect to the value in isotopically pure lattices due to the strong reduction of the phonon mean-free path.[20] Close inspection of our results reveals that thermal conductivity of nanotubes remains almost unaffected by the presence of ^{13}C
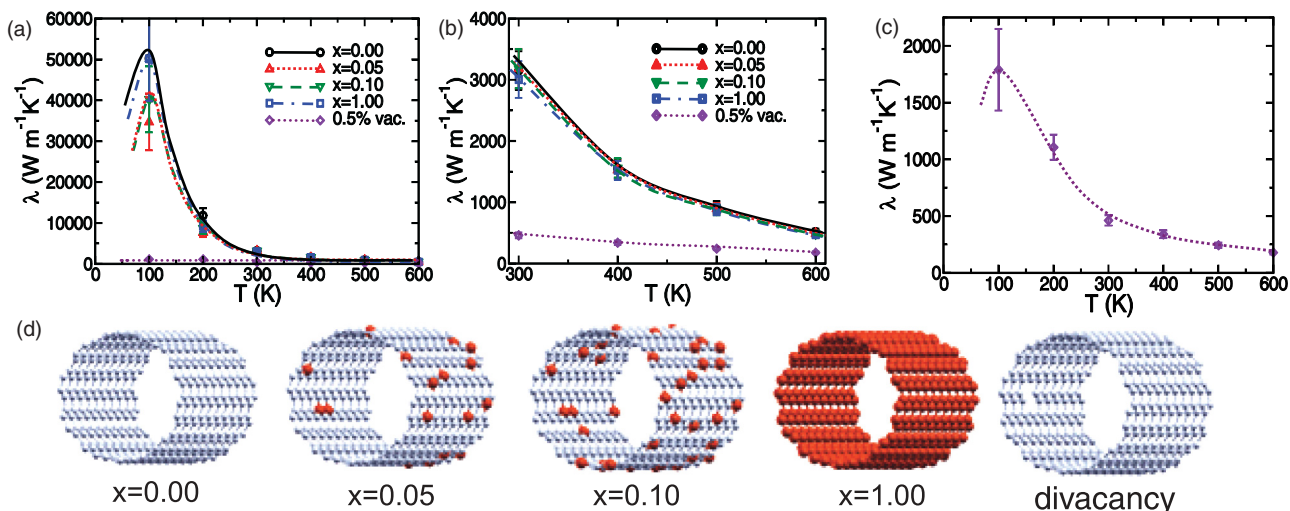
FIG. 1. (Color online) Thermal conductivity λ of perfect and defective (10,10) carbon nanotubes as a function of temperature T. (a) λ in structurally perfect $^{13}C_x{}^{12}C_{1-x}$ nanotubes with varying isotopic composition in comparison to pure ^{12}C nanotubes with 0.5% missing atoms forming divacancy defects. (b) Details of (a) on a reduced temperature scale. (c) λ of ^{12}C nanotubes with divacancies, presented in (a) and (b), on an expanded λ scale. (d) Depiction of the nanotube unit cell containing different types of defects. The lines in (a)–(c) are guides to the eye.

isotopic impurities at temperatures $T \gtrsim 300$ K, where phonon-phonon scattering seems to dominate the mean-free-path reduction.

To find out the relative importance of isotopic impurities and structural defects, we also studied thermal conductivity in isotopically pure ^{12}C (10,10) nanotubes containing a small fraction of atomic vacancies. We focused on divacancies, which are more stable than monatomic vacancies,[29,30] and considered one single divacancy per 400-atom unit cell. Our results for λ in this system, shown in Figs. 1(a)–1(c), indicate that even a very low concentration of structural defects may quench thermal conductivity by roughly an order of magnitude. These results support our intuition that vacancies scatter phonons very efficiently and reduce the phonon mean-free path even more than isotopic impurities. Whereas the reduction of λ by 97% at $T \approx 100$ K is extremely large, the relative role of structural defects decreases at higher temperatures, reaching a value of 83% at 300 K and 67% at 600 K. In accord with our

findings for isotope mixtures, we conclude that mean-free-path reduction by phonon-phonon scattering starts dominating the adverse effect of defects at high temperatures.

B. Thermal conductivity of graphene

Due to the present interest in graphene, we determined the influence of defects on its thermal conductivity and present our results in Fig. 2. Results for λ in structurally perfect, free-standing infinite graphene monolayers with the isotopic composition $^{13}C_x{}^{12}C_{1-x}$ are shown in Figs. 2(a) and 2(b) for a selected set of compositions in the temperature range up to 600 K. Graphene monolayers were represented by a periodic array of rectangular 180-atom unit cells. As in the case of nanotubes, isotopically pure graphene has the highest thermal conductivity. Similar to nanotubes, the maximum value of λ is reached near $T \approx 100$ K.
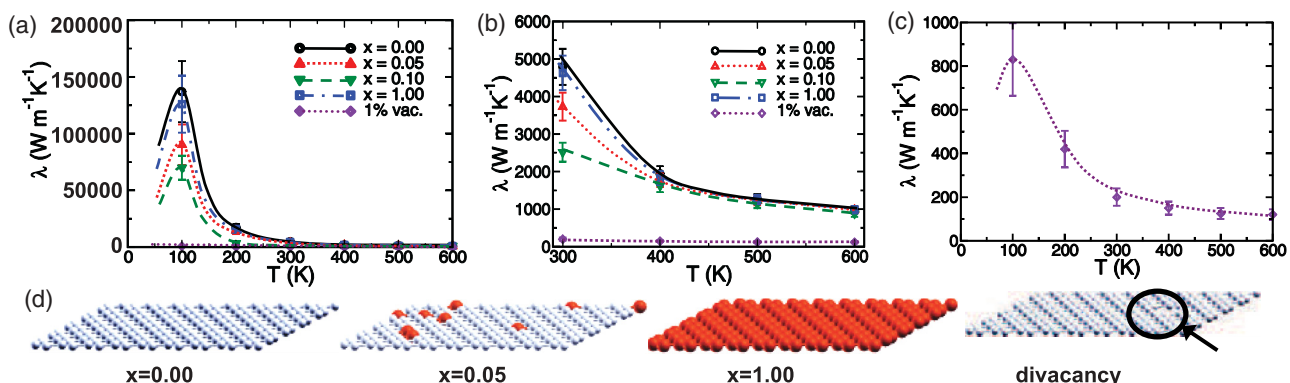

FIG. 2. (Color online) Thermal conductivity λ of perfect and defective graphene and graphene nanoribbons as a function of temperature T. (a) λ in $^{13}C_x{}^{12}C_{1-x}$ graphene with varying isotopic composition in comparison to pure ^{12}C graphene with 1% missing atoms forming divacancy defects. (b) Details of (a) on a reduced temperature scale. (c) λ of ^{12}C graphene with divacancies, presented in (a) and (b), on an expanded λ scale. (d) Depiction of the graphene unit cells containing different types of defects. The lines in (a)–(c) are guides to the eye.

We find the thermal conductivity to be slightly higher in defect-free graphene consisting of ^{12}C than of ^{13}C. In contrast to nanotubes, the reduction of the thermal conductivity in isotopic mixtures is much more pronounced in graphene. Whereas a 10% content of ^{13}C isotopic impurities reduced the thermal conductivity at 100 K by 30% in nanotubes, the corresponding 50% reduction in graphene is much larger. This is consistent with the fact that in defect-free systems, phonon-phonon scattering limits the phonon mean-free path more in nanotubes with a finite circumference than in graphene. Similar to nanotubes, the presence of a single divacancy per unit cell quenches the thermal conductivity by more than an order of magnitude, as seen in Figs. 2(a)–2(c). Also in graphene, the reduction of the thermal conductivity due to isotopic and structural defects is mainly caused by the decrease in the phonon mean-free path.

C. Thermal conductivity of graphene nanorribons

Finally, we compared thermal conductivity of graphene to that of 11.1-Å-wide armchair graphene nanoribbons, using the same ^{13}C$_x$^{12}C$_{1-x}$ isotopic compositions as for graphene and nanotubes. The nanoribbons were represented using periodic boundary conditions using 131.5-Å-long unit cells containing 600 C atoms. Our results for the thermal conductivity of nanoribbons are presented in Fig. 3.

Our results for finite-width nanoribbons should be very relevant also for graphene formed by chemical vapor deposition (CVD). Grain boundaries in CVD graphene, viewed as lines of incorrectly coordinated carbon atoms, will scatter phonons and limit thermal conductivity in a very similar way as nanoribbon edges. Since the unit-cell size representing realistic grain boundaries is prohibitively large for atomistic simulations, we only point out the analogy between nanoribbons and polycrystalline graphene. For isotopically pure ^{12}C-based systems, comparison between λ of graphene in Fig. 2(a) and graphene nanoribbons in Fig. 3 reveals that edges in nanoribbons quench thermal conductivity in a much more

drastic way than sparse diatomic vacancies in an infinite graphene monolayer. We observe reduction of λ by a factor of 700 at $T = 100$ K, a factor of 30 at 300 K, and by an order of magnitude at 600 K.

Possibly unexpected at the first glance is our finding that placing one divacancy per 600-atom unit cell, corresponding to 0.33% atomic vacancies, does not cause as drastic a reduction of the thermal conductivity as in the case of nanotubes and graphene. Whereas this effect is still significant at low temperatures, amounting to a 60% reduction at $T = 100$ K, it becomes negligibly small at temperatures above 400 K. We conclude that the underlying reduction of the phonon mean-free path in narrow graphene nanoribbons is dominated by the presence of edges and that additional structural defects play only a minor role, especially at higher temperatures. Due to the dominating role of edges as scattering centers in nanoribbons, the role of isotopic impurities is much smaller in these systems than in nanotubes and graphene. Still, in agreement with our results for nanotubes and graphene, we find that isotopically pure nanoribbons based on ^{12}C conduct heat slightly better than those based on ^{13}C.

D. High-temperature behavior

Even though infinitely extended graphene appears to conduct heat better than nanotubes at low temperatures, the difference between the two systems becomes smaller at 400 K and above. As already mentioned above, the adverse effect of defects on the thermal conductivity of carbon nanostructures becomes less significant at higher temperatures, when uncorrelated atomic motion reduces the phonon mean-free path even in defect-free systems. In practice, we find very similar thermal conductivities in isotopically pure systems and in isotope mixtures at very high temperatures $T \gtrsim 600$ K. At still higher temperatures approaching the melting point, when vacancy production occurs naturally, presence of additional structural defects should play a negligible role as well. At those high temperatures, thermal conductivity of nanotubes and graphene may drop close to that of nanoribbons.
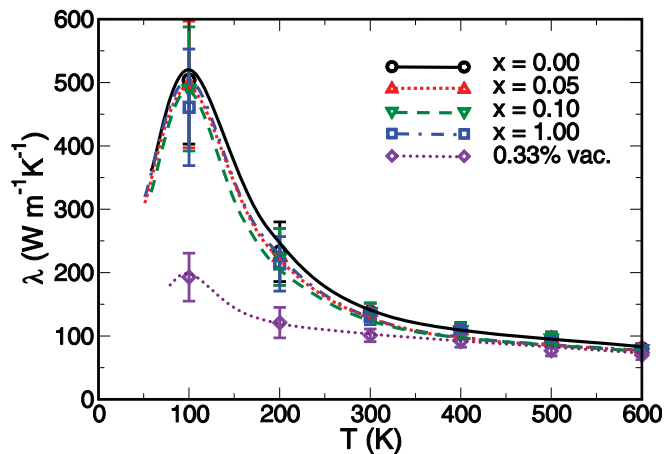
IV. SUMMARY AND CONCLUSIONS

In conclusion, we studied the adverse role of defects on the thermal conductivity of carbon nanotubes, graphene, and graphene nanoribbons using nonequilibrium molecular dynamics simulations. We found that all defects, including divacancies, extended edges and isotopic impurities reduce thermal conductivity significantly in all systems by introducing phonon scattering centers and thus decreasing the phonon mean-free path. We reconciled results of former studies, which differed by up to an order of magnitude, by identifying limitations of various computational approaches. We found that infinite, defect-free graphene should conduct heat better than any other carbon nanostructure at low temperatures. For temperatures $T \lesssim 400$ K, isotopic impurities were found to quench the thermal conductivity of graphene more than that of carbon nanotubes. We found that even subpercent concentrations of divacancies reduced the thermal conductivity of all nanocarbons more than much higher concentrations of isotopic impurities. For temperatures $T \lesssim 400$ K, the adverse effect of divacancies was found to be more pronounced in

FIG. 3. (Color online) Temperature dependence of the thermal conductivity λ of ^{13}C$_x$^{12}C$_{1-x}$ structurally perfect graphene nanoribbons in comparison to pure ^{12}C graphene nanoribbons with 0.33% missing atoms arranged as divacancies. The lines are guides to the eye.

graphene than in carbon nanotubes. Finite-width graphene nanoribbons can be viewed as graphene with extended vacancies and thus have not only a much lower thermal conductivity, but also a lower susceptibility to the presence of additional defects than graphene. At high temperatures, when anharmonicities in the force field reduce the phonon mean-free path more than defects, we find that thermal conductivity decreases significantly and that differences between particular nanocarbons become washed out to a large degree.

*tomanek@pa.msu.edu

[1] E. Pop, S. Sinha, and K. Goodson, Proc. IEEE **94**, 1587 (2006).

[2] L. Wei, P. K. Kuo, R. L. Thomas, T. R. Anthony, and W. F. Banholzer, Phys. Rev. Lett. **70**, 3764 (1993).

[3] T. R. Anthony, W. F. Banholzer, J. F. Fleischer, L. Wei, P. K. Kuo, R. L. Thomas, and R. W. Pryor, Phys. Rev. B **42**, 1104 (1990).

[4] S. Berber, Y.-K. Kwon, and D. Tomanek, Phys. Rev. Lett. **84**, 4613 (2000).

[5] A. A. Balandin, Nat. Mater. **10**, 569 (2011).

[6] S. Chen, Q. Wu, C. Mishra, J. Kang, H. Zhang, K. Cho, W. Cai, A. A. Balandin, and R. S. Ruoff, Nat. Mater. **11**, 203 (2012).

[7] P. Zhao, E. Einarsson, R. Xiang, Y. Murakami, S. Chiashi, J. Shiomi, and S. Maruyama, Appl. Phys. Lett. **99**, 093104 (2011).

[8] A. Maeda and T. Munakata, Phys. Rev. E **52**, 234 (1995).

[9] D. J. Evans, Phys. Lett. A **91**, 457 (1982).

[10] D. P. Hansen and D. J. Evans, Mol. Phys. **81**, 767 (1994).

[11] M. J. Gillan and M. Dixon, J. Phys. C: Solid State Phys. **16**, 869 (1983).

[12] P. K. Schelling, S. R. Phillpot, and P. Keblinski, Phys. Rev. B **65**, 144306 (2002).

[13] D. A. McQuarrie, *Statistical Mechanics* (Harper & Row, London, 1976).

[14] H. Zhang, G. Lee, and K. Cho, Phys. Rev. B **84**, 115460 (2011).

[15] J. Shiomi and S. Maruyama, Phys. Rev. B **74**, 155401 (2006).

[16] J.-W. Jiang, J. Lan, J.-S. Wang, and B. Li, J. Appl. Phys. **107**, 054314 (2010).

[17] W. Zhang, Z. Zhu, F. Wang, T. Wang, L. Sun, and Z. Wang, Nanotechnology **15**, 936 (2004).

[18] M. Grujicic, G. Cao, and W. N. Roy, J. Mater. Sci. **40**, 1943 (2005).

[19] H. Zhang, G. Lee, A. F. Fonseca, T. L. Borders, and K. Cho, J. Nanomater. **2010**, 537657 (2010).

[20] I. Savić, N. Mingo, and D. A. Stewart, Phys. Rev. Lett. **101**, 165502 (2008).

[21] J. Wang, L. Li, and J.-S. Wang, Appl. Phys. Lett. **99**, 091905 (2011).

[22] D. C. Rapaport, *The Art of Molecular Dynamics Simulation* (Cambridge University Press, Cambridge, 1998).

[23] J. Tersoff, Phys. Rev. Lett. **61**, 2879 (1988).

[24] See Supplemental Material at http://link.aps.org/supplemental/10.1103/PhysRevB.86.125418 for the vibrational spectra of graphene obtained using the Tersoff potential and *ab initio* density functional calculations.

[25] S. Nosé, J. Chem. Phys. **81**, 511 (1984).

[26] W. G. Hoover, Phys. Rev. A **31**, 1695 (1985).

[27] Converged results for the thermal conductivity of graphene based on the Green-Kubo formalism require simulation times of possibly more than 1 ns for each ensemble (Ref. 14). This is one order of magnitude longer than what is required for a nonequilibrium molecular dynamics simulation.

[28] C. W. Gear, Argonne National Laboratory Report No. 7126, 1966 (unpublished).

[29] F. Banhart, J. Kotakoski, and A. V. Krasheninnikov, ACS Nano **5**, 26 (2011).

[30] S. Berber and A. Oshiyama, Phys. Rev. B **77**, 165405 (2008).